



# Molecular Crystals and Liquid Crystals Science and Technology. Section A. Molecular Crystals and Liquid Crystals

Publication details, including instructions for authors and subscription information:

<http://www.tandfonline.com/loi/gmcl19>

## Ferroelectric-Like and Antiferroelectric-Like Behaviour of the $\text{SmC}_\alpha^*$ Phase

Sandra Sarmento <sup>a</sup>, Paulo Simeão Carvalho <sup>a</sup>,  
 Maria Renata Chaves <sup>a</sup>, Huu Tinh Nguyen <sup>b</sup> & Filipa Pinto <sup>a</sup>

<sup>a</sup> Departamento de Física, IMAT (núcleo IFIMUP),  
 CFUP, Faculdade de Ciências da Universidade do  
 Port, R. do Campo Alegre, 687, 4150, Porto, Portugal

<sup>b</sup> Centre de Recherche Paul Pascal, Av. A.  
 Schweitzer, 33600, Pessac, France

Version of record first published: 24 Sep 2006

To cite this article: Sandra Sarmento, Paulo Simeão Carvalho, Maria Renata Chaves, Huu Tinh Nguyen & Filipa Pinto (1999): Ferroelectric-Like and Antiferroelectric-Like Behaviour of the  $\text{SmC}_\alpha^*$  Phase, Molecular Crystals and Liquid Crystals Science and Technology. Section A. Molecular Crystals and Liquid Crystals, 328:1, 457-465

To link to this article: <http://dx.doi.org/10.1080/10587259908026089>

Full terms and conditions of use: <http://www.tandfonline.com/page/terms-and-conditions>

This article may be used for research, teaching, and private study purposes. Any substantial or systematic reproduction, redistribution, reselling, loan, sub-licensing, systematic supply, or distribution in any form to anyone is expressly forbidden.

The publisher does not give any warranty express or implied or make any representation that the contents will be complete or accurate or up to date. The accuracy of any instructions, formulae, and drug doses should be independently verified with primary sources. The publisher shall not be liable for any loss, actions, claims, proceedings, demand, or costs or damages whatsoever or howsoever caused arising directly or indirectly in connection with or arising out of the use of this material.

## Ferroelectric-Like and Antiferroelectric-Like Behaviour of the $\text{SmC}_\alpha^*$ Phase

SANDRA SARMENTO<sup>a</sup>, PAULO SIMEÃO CARVALHO<sup>a</sup>, MARIA RENATA CHAVES<sup>a</sup>, HUU TINH NGUYEN<sup>b</sup> and FILIPA PINTO<sup>a</sup>

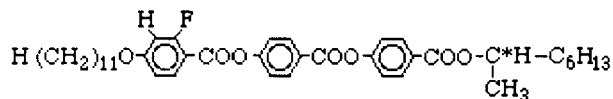
<sup>a</sup>*Departamento de Física, IMAT (núcleo IFIMUP), CFUP, Faculdade de Ciências da Universidade do Porto, R. do Campo Alegre, 687, 4150 Porto, Portugal*  
 and <sup>b</sup>*Centre de Recherche Paul Pascal, Av. A. Schweitzer, 33600 Pessac, France*

This work describes an extensive study of the compound 11HFBBBM7<sup>[1]</sup>, which presents the  $\text{SmC}_\alpha^*$  phase in a relatively large temperature interval ( $\approx 3.3^\circ\text{C}$ ). The polarization hysteresis loops obtained at stabilized temperatures disclosed an antiferroelectric behaviour in the high temperature range of the  $\text{SmC}_\alpha^*$  phase. Dielectric dispersion was studied as a function of the bias field.

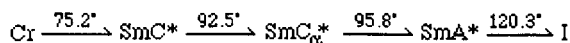
**Keywords:**  $\text{SmC}_\alpha^*$  phase; antiferroelectric; bias field; hysteresis loops

### INTRODUCTION

The compound studied presents the chemical formula<sup>[1]</sup>:



Differential Scanning Calorimetry (DSC) and optical observations of planar and homeotropic samples suggested the following phase sequence<sup>[1]</sup>:



Both the  $\text{SmA}^*$  and the  $\text{SmC}^*$  phases have been extensively studied, and there is good experimental evidence to support the accepted models that describe their structures and properties. The structure of the  $\text{SmC}_\alpha^*$  phase is

rather complex and it is not fully understood yet. Sophisticated models have been proposed<sup>[2,3]</sup>, taking into account the main features of the experimental data obtained so far. Recent X-ray results indicate an incommensurate periodicity, evolving from 5 to 8 smectic layers with increasing temperature, in the  $\text{SmC}_\alpha^*$  phase<sup>[4]</sup>. Usually, this phase is stable in a short temperature interval ( $\approx 1$  K), which makes its experimental study difficult. As in our compound the  $\text{SmC}_\alpha^*$  phase is stable in a rather large temperature interval ( $\approx 3.3$  K), we have studied its dielectric properties as a function of the bias electric field to obtain a better understanding of this phase.

## EXPERIMENTAL

All measurements were performed on planar, 25  $\mu\text{m}$  thick samples, prepared from commercial cells of E.H.C. Co - Japan. To control and measure the temperature, we used the setup described in reference<sup>[5]</sup>, which has an accuracy better than 0.1 K. All the results presented were obtained on heating.

The phase sequence, determined by DSC, was confirmed with the TSM (Temperature Scan Method) technique<sup>[6]</sup>. Polarization hysteresis loops were obtained using a sinusoidal wave (frequency 20-50 Hz) from a HP33120A generator, amplified by a Kepko amplifier (model BOP 1000M).

Dielectric dispersion was studied as a function of the bias field, in the frequency range 20 Hz to 1 MHz, with a measuring a.c. field of 0.1  $\text{kVcm}^{-1}$ . The data were fitted to the expression<sup>[7]</sup>:

$$\varepsilon^*(\omega) = \varepsilon_\infty + \frac{1}{i f/f_c} + \sum_j \frac{\Delta\varepsilon_j}{1 + (i f/f_{Rj})^{\beta_j}} \quad (1)$$

where the second term accounts for the conductivity of the sample,  $\Delta\varepsilon_j$  is the dielectric amplitude of mode  $j$  and the corresponding parameter  $\beta_j$  measures the dispersion of the characteristic relaxation time ( $\tau_{Rj} = 1/f_{Rj}$ ).

## EXPERIMENTAL RESULTS AND DISCUSSION

### TSM Measurements

The  $\text{SmC}^*$ - $\text{SmC}_\alpha^*$  and  $\text{SmC}_\alpha^*$ - $\text{SmA}^*$  phase transitions were detected by

TSM, and the corresponding temperatures were found to be independent of the measuring field up to  $20 \text{ kVcm}^{-1}$ . For stronger fields, the  $\text{SmC}^*-\text{SmC}_\alpha^*$  phase transition is not seen. A similar result was obtained on thiobenzoate series[8]. Measurements on cooling and heating runs revealed a thermal hysteresis of less than 1 K for the  $\text{SmC}^*-\text{SmC}_\alpha^*$  and for the  $\text{SmC}_\alpha^*-\text{SmA}^*$  phase transitions.

### Polarization Hysteresis Loops

The polarization in the unwound state ( $P_s$ ) and the spontaneous tilt angle ( $\theta_s$ ) were deduced from polarization and optical hysteresis loops, respectively. These two quantities present no discontinuities at the  $\text{SmC}^*-\text{SmC}_\alpha^*$  phase transition. At  $\approx 80^\circ\text{C}$ ,  $\theta_s$  is  $\approx 21^\circ$  and  $P_s$  is  $\approx 57 \text{ nCcm}^{-2}$ .

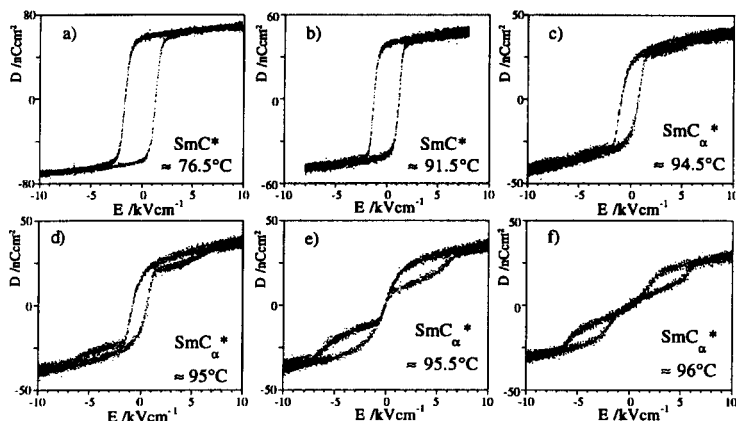


FIGURE 1 Polarization hysteresis loops in the  $\text{SmC}^*$  and  $\text{SmC}_\alpha^*$  phases.

Figure 1 presents polarization hysteresis loops obtained at some stabilized temperatures. In the  $\text{SmC}^*$  phase, we have obtained single hysteresis loops, typical of a ferroelectric phase. In the low temperature range of this phase the saturation field is  $\approx 4 \text{ kVcm}^{-1}$ . As expected, it decreases with increasing temperature and at  $\approx 91.5^\circ\text{C}$  it is only  $\approx 2 \text{ kVcm}^{-1}$  (see figures 1(a) and 1(b)).

In the low temperature range of the  $\text{SmC}_\alpha^*$  phase the loops are ferroelectric-like, as seen in figure 1(c). However, a hint of two other loops can be guessed for  $|E| \approx 2 \text{ kVcm}^{-1}$  in this figure. At intermediate temperatures the

hysteresis loops observed are rather complex (see figure 1(d)), and triple loops can be seen. Near the transition to the SmA\* phase, double hysteresis loops are observed (see figures 1(e) and 1(f)), which are often related to an antiferroelectric behaviour. This change from ferroelectric-like to antiferroelectric-like behaviour may be due to a change in the structure of the phase, as predicted by some models<sup>[2,3]</sup>. The evolution of the polar behaviour with temperature within the SmC $\alpha$ \* phase is in agreement with that observed in thiobenzoate compounds with a fluoro substituent<sup>[5,9]</sup>.

In the high temperature range of the SmC $\alpha$ \* phase the saturation field ( $\approx 6 \text{ kVcm}^{-1}$  at  $\approx 96^\circ\text{C}$ ) is much higher than it was found in the SmC\* phase. Such an increase of the saturation field is due to a decrease of the helical pitch. As it is well known, for a smaller pitch the elastic energy of the helix increases.

### **Dielectric Dispersion Measurements**

The dielectric dispersion was studied as a function of the temperature for different values of the bias field (figure 2). The usual effect of the ITO electrodes was always observed at  $\approx 1 \text{ MHz}$ <sup>[7]</sup>. Below this frequency, only one relaxation mode was detected at each temperature.

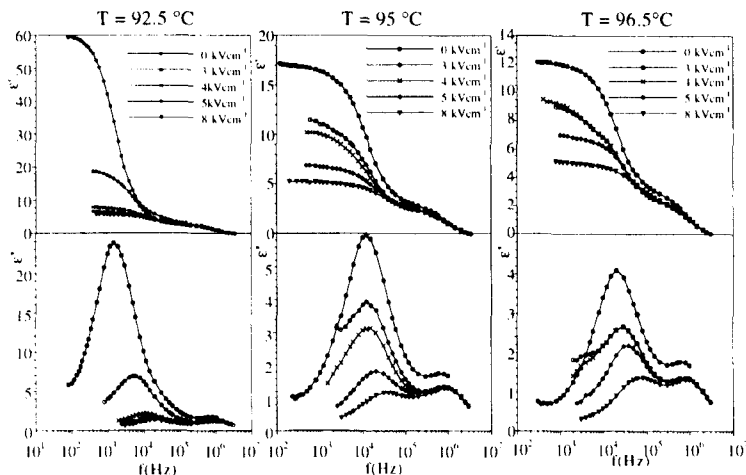


FIGURE 2  $\epsilon'(f)$  and  $\epsilon''(f)$  curves, obtained at different temperatures under different values of bias field.

The curves of  $\epsilon'(f)$  and  $\epsilon''(f)$  were fitted simultaneously using expression (1) and the parameters  $\Delta\epsilon$ ,  $f_R$  and  $\beta$  were obtained. The temperature dependence of  $\Delta\epsilon$  is displayed in figure 3(a), for different values of the bias field. The portion outlined with a rectangle in this figure is presented in detail in figure 3(b). The parameters  $f_R(T)$ ,  $1/\Delta\epsilon(T)$  and  $\beta(T)$  (presented, respectively, in figures 4(a), 4(b) and 4(c), for different bias fields) were found to behave very differently in the  $\text{SmC}^*$ ,  $\text{SmC}_\alpha^*$  and  $\text{SmA}^*$  phases.

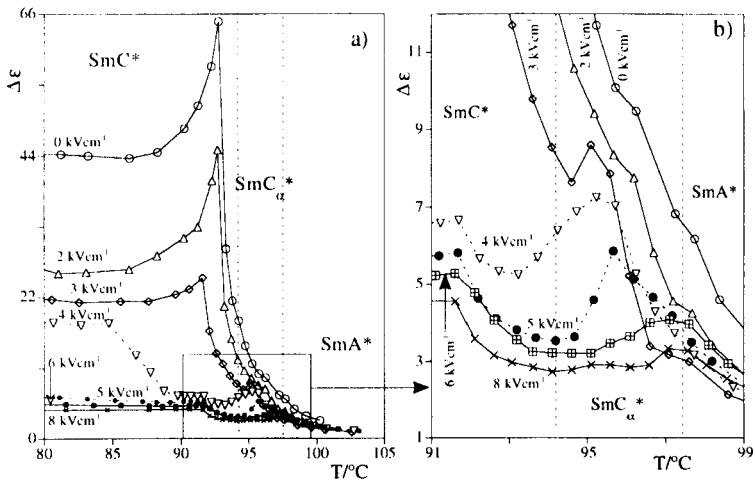


FIGURE 3 (a) Dielectric amplitude as a function of the temperature and the applied bias field. (b) Detail of figure 3(a) corresponding to the inside of the rectangle.

### The $\text{SmC}^*$ phase

By admitting the usual helicoidal structure for the  $\text{SmC}^*$  phase, two low frequency relaxation modes are expected: the Goldstone mode and the soft mode. It is habitually verified that  $\Delta\epsilon_G \propto (p/P_s/\theta_s)^2$ , where  $p$  is the helical pitch and  $1/\Delta\epsilon_S \propto (T^*-T)$ . These relations are obtained from a Landau expansion of the free energy, for a  $\text{SmC}^*$ - $\text{SmA}^*$  phase transition<sup>[10]</sup>. In our experiment, the soft mode was never observed in the  $\text{SmC}^*$  phase, even for a bias field strong enough to unwind the helix and to eliminate the Goldstone mode.

In the absence of bias field, the relaxation process observed is the Goldstone mode.  $f_R(T)$  presents a minimum and  $\Delta\epsilon(T)$  a maximum at 92.6°C, i. e., 1.6°C below the  $\text{SmC}^*-\text{SmC}_\alpha^*$  phase transition. This behaviour very probably reflects the temperature dependence of  $p$ , since the quantity  $P_s/\theta_s$  was found to decrease smoothly and linearly throughout the  $\text{SmC}^*$  phase.

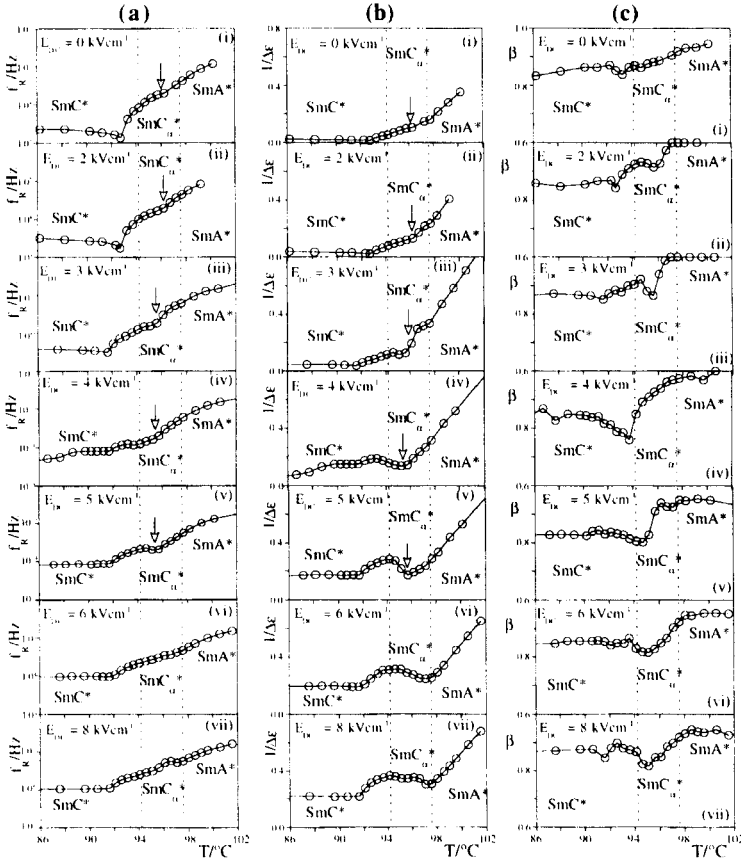


FIGURE 4 Temperature dependence of (a)  $f_R$  (b)  $1/\Delta\epsilon$  and (c)  $\beta$  for different bias electric fields.



The bias field causes  $\Delta\epsilon(T)$  to decrease and  $f_R(T)$  to increase (see figures 3(a) and 4(a)). The results also indicate that the temperature behaviour of  $\Delta\epsilon$  and  $f_R$  at high bias field ( $E_{dc} \geq 5 \text{ kVcm}^{-1}$ ) is significantly different from that observed for  $E_{dc} \leq 2 \text{ kVcm}^{-1}$  and that the effect of the bias field is very strong in the  $\text{SmC}^*$  phase and near the  $\text{SmC}^*-\text{SmC}_\alpha^*$  phase transition.

As the hysteresis loops are always saturated above  $4 \text{ kVcm}^{-1}$ , indicating in this way the complete unwinding of the helical structure, the relaxation process observed for  $E_{dc} > 4 \text{ kVcm}^{-1}$  does not correspond to the Goldstone mode. Its nature is not understood yet, but it can be related to surface phenomena, since polarizing microscopy revealed a texture with many defects.

The dispersion parameter,  $\beta(T)$  is  $\approx 0.85$  in the  $\text{SmC}^*$  phase, indicating a polydisperse behaviour. The temperature dependence of this parameter is approximately constant and not greatly influenced by the bias field.

### The $\text{SmC}_\alpha^*$ phase

Figure 4 shows that  $1/\Delta\epsilon(T)$ ,  $f_R(T)$  and  $\beta(T)$  change continuously with the temperature at the  $\text{SmC}^*-\text{SmC}_\alpha^*$  and  $\text{SmC}_\alpha^*-\text{SmA}^*$  phase transitions. As shown in figure 4(c), the relaxation mode detected in the  $\text{SmC}_\alpha^*$  phase is polydisperse, and the temperature behaviour of  $\beta$  is strongly influenced by the bias field.

The  $f_R(T)$  and  $1/\Delta\epsilon(T)$  curves obtained without bias field present an anomaly at  $\approx 96^\circ\text{C}$ , indicated by arrows in figures 4(a)(i) and 4(b)(i). We admit that this behaviour is related to the anomalies in the helical pitch, detected within this phase by V. Laux et al<sup>[11]</sup> (the inversion of the helix was detected on cooling for this compound). Increasing the bias field, that anomaly is enhanced and shifted to lower temperatures, as seen in figures 4(a) and 4(b). It corresponds to the local maximum of  $\Delta\epsilon$  observed in the  $\text{SmC}_\alpha^*$  phase in figure 3(b). This behaviour must be related to the Goldstone mode contribution. In fact, for  $E_{dc} > 2 \text{ kVcm}^{-1}$  the helix is unwound in the high temperature range of the  $\text{SmC}^*$  phase, but it is surely present in the  $\text{SmC}_\alpha^*$  phase up to the value of the saturation field ( $\approx 6 \text{ kVcm}^{-1}$ ). Therefore, in the  $\text{SmC}_\alpha^*$  phase,  $\Delta\epsilon(T)$  reflects the temperature dependence of the helical pitch, for  $E_{dc} < 6 \text{ kVcm}^{-1}$ .

For  $E_{dc} \geq 6 \text{ kVcm}^{-1}$ , the helix is suppressed in the whole temperature range of the  $\text{SmC}_{\alpha}^*$  phase.  $\Delta\epsilon$  presents a maximum at the transition to the  $\text{SmA}^*$  phase due to the softening of the soft mode (see figures 3(b) and 4(b)(vii)).

### The $\text{SmA}^*$ phase

In the  $\text{SmA}^*$  phase, the Landau theory predicts a Curie Weiss behaviour for the soft mode, i. e.,  $1/\Delta\epsilon_S \propto (T-T^*)$ , where  $T^* = T_C - \Delta T$  ( $\Delta T > 0$ ) and  $T_C$  is the temperature where the  $\text{SmC}_{\alpha}^*$ - $\text{SmA}^*$  phase transition occurs<sup>[10]</sup>.  $1/\Delta\epsilon$  versus  $T$  is depicted in figure 4(b) and its behaviour in this phase is in close agreement with the theory, for all values of the bias field. The temperature  $T_C$  is not changed by the field, but  $T^*$  decreases linearly with increasing field:  $T^*(E_{dc} = 0) = 95.8^\circ\text{C}$  while  $T^*(E_{dc} = 8 \text{ kVcm}^{-1}) = 94.6^\circ\text{C}$ . Consequently,  $\Delta T$  increases with the field.

In the absence of bias field, the  $\beta$  parameter is  $\approx 0.95$  in the  $\text{SmA}^*$  phase, as shown in figure 4(c)(i). However, for low values of bias (up to  $4 \text{ kVcm}^{-1}$ ), the soft mode becomes monodispersive ( $\beta = 1$ ), reflecting a higher degree of order imposed by the field (see figures 4(c) (ii) to (iv)). Unexpectedly, for higher fields, the  $\beta$  parameter decreases as seen in figures 4(c) (v) to (vii), maybe owing to some competitive effect enhanced by the bias field.

## CONCLUSIONS

Polarization hysteresis loops revealed a ferroelectric-like behaviour in the low temperature range of the  $\text{SmC}_{\alpha}^*$  phase, becoming antiferroelectric-like near the transition to the  $\text{SmA}^*$  phase.

In the  $\text{SmC}^*$  and  $\text{SmC}_{\alpha}^*$  phases, the  $f_R(T)$ ,  $\Delta\epsilon(T)$  and  $\beta(T)$  curves are strongly influenced by the applied bias field. In the  $\text{SmC}_{\alpha}^*$  phase the electric field needed to unwind the helix is higher than in the  $\text{SmC}^*$  phase, as the helical pitch is larger in this phase than in the  $\text{SmC}_{\alpha}^*$  phase. Under a bias field high enough to suppress the Goldstone mode, a relaxation process was disclosed in the  $\text{SmC}^*$  phase. Its nature is not identified, but it may be related to surface effects.

### Acknowledgments

The authors are grateful to Albano Costa for technical assistance and to Dr. M. Glogarová for useful discussions. This work was supported by the project PRAXIS XXI /3 /3.1 /MMA /1769 /95. S. Sarmento and F. Pinto thank project PRAXIS XXI for their grants (respectively BD /9545 /96 and BIC J /4688/96).

## References

- [1] V. Faye, J.C. Rouillon, C. Destrade and H.T. Nguyen, *Liq. Cryst.*, **19**, 47 (1995).
- [2] Y. Takamishi, K. Hiraoka, V. Agrawal, H. Takezoe, A. Fukuda and M. Matsushita, *Jpn. J. Appl. Phys.*, **30**, 2023 (1991).
- [3] M. Cepic and B. Zecks, *Mol. Cryst. Liq. Cryst.*, **263**, 61 (1995).
- [4] P. Mach, R. Pindak, A.M. Levelut, P. Barois, H.T. Nguyen, C.C. Huang and L. Furen-  
lid, to be published in *Phys. Rev. Lett.*
- [5] P. Simeão Carvalho, M.R. Chaves, C. Destrade, H.T. Nguyen and M. Glogarová, *Liq. Cryst.*, **21**, 31 (1996).
- [6] P. Simeão Carvalho, M. Glogarová M.R. Chaves, C. Destrade, and H.T. Nguyen, *Liq. Cryst.*, **21**, 115 (1996).
- [7] F. Gouda, K. Skarp and S.T. Lagerwall, *Ferroelectrics*, **113**, 165 (1991).
- [8] P. Simeão Carvalho, S. Sarmento, M.R. Chaves, H.T. Nguyen, to be published.
- [9] P. Simeão Carvalho, M. Glogarová. M.R. Chaves, H.T. Nguyen, C. Destrade, J.C. Rouillon, S. Sarmento, M.J. Ribeiro, *Liq. Cryst.*, **21**, 511 (1996).
- [10] J.W. Goodby, R. Blinc, N.A. Clark, S.T. Lagerwall, M.A. Osipov, S.A. Pikin, T. Sakurai, K. Yoshino, B. Zecks, in *Ferroelectric liquid Crystals-Principles, Properties and Applications – FERROELECTRICITY AND RELATED PHENOMENA – VOL-UME 7*, Chap.V, (Gordon and Breach, Amsterdam, 1991).
- [11] Valérie Laux, University of Lille I, Ph.D. thesis, 109, (1997).